Space Weather

RESEARCH ARTICLE
10.1029/2021SW002944

# Investigating Effects of Solar Proton Events and Forbush Decreases on Ground-Level Potential Gradient Recorded at Middle and Low Latitudes and Different Altitudes

**J. Tacza[1,2], A. Odzimek[1], E. Tueros Cuadros[3], J.-P. Raulin[2], M. Kubicki[1], G. Fernandez[4], and A. Marun[5]**

[1]Institute of Geophysics, Polish Academy of Sciences, Warsaw, Poland, [2]Center of Radio Astronomy and Astrophysics Mackenzie, Engineering School, Mackenzie Presbyterian University, Sao Paulo, Brazil, [3]National Institute for Space Research, Sao Jose dos Campos, Brazil, [4]Complejo Astronomico El Leoncito, CASLEO, San Juan, Argentina, [5]Instituto de Ciencias Astronomicas de la Tierra y el Espacio, ICATE-CONICET-UNSJ, San Juan, Argentina

**Key Points:**

- Intense solar proton events increase the potential gradient in fair weather conditions at high altitude stations
- Strong Forbush decrease enhance the potential gradient in fair weather conditions at high altitude stations
- Ground level enhancement can produce changes on the potential gradient in fair weather conditions at high altitude stations

**Correspondence to:**
J. Tacza,
josect1986@gmail.com

**Citation:**
Tacza, J., Odzimek, A., Tueros Cuadros, E., Raulin, J.-P., Kubicki, M., Fernandez, G., & Marun, A. (2022). Investigating effects of solar proton events and Forbush decreases on ground-level potential gradient recorded at middle and low latitudes and different altitudes. *Space Weather*, *20*, e2021SW002944. https://doi.org/10.1029/2021SW002944

Received 5 OCT 2021
Accepted 21 FEB 2022

**Abstract** High-energetic charged particles, such as solar protons, and phenomena such as Forbush decreases are eligible candidates to affect the global electric circuit. These effects have been studied by analyzing disturbances of the potential gradient in ground-based measurements in fair weather regions. In this paper, we investigate deviations in the potential gradient diurnal curve, during solar proton events, and Forbush decreases, from the mean values obtained in fair weather conditions. In each situation, we select only events which are not accompanied or followed by the other. Using the superposed epoch analysis, in order to enhance the visualization of small effects, we study the potential gradient data recorded between January 2010 and December 2019 at two stations located at low and middle-latitudes, and at two different altitudes: the Complejo Astronómico El Leoncito (CASLEO), Argentina: 31.78°S, 2550 m a.s.l., and the Geophysical Observatory in Świder (SWIDER), Poland: 52.12°N, 100 m a.s.l., respectively. For intense solar proton events (>100 MeV) we found a statistically significant increase of the potential gradient after solar proton events recorded at CASLEO and no such deviation in the potential gradient recorded at SWIDER. For Forbush decrease events (greater than 4%), no significant deviation of the potential gradient after the start of the event was found in both stations, however for very intense Forbush decreases (>7%) we found an increase of the potential gradient recorded at CASLEO.

**Plain Language Summary** The Earth's atmosphere is constantly bombarded by highly energetic charged particles from the Sun, our galaxy and other galaxies. These energetic charged particles interact with the particles of the Earth's atmosphere affecting our environment. In this study, we focus on the impact of solar proton events (high solar energetic charged particles) and Forbush Decreases (suppression of energetic charged particle flux), on the Earth's electrical activity. Particularly, we evaluate the impact of these phenomena in the atmospheric electric field (or potential gradient) recorded at ground level in two different stations located at different latitudes and at different altitudes. Our results show that the potential gradient is especially sensitive to solar proton events and Forbush Decrease at Complejo Astronómico El Leoncito station located at high altitude.

## 1. Introduction

The Earth's atmosphere is constantly bombarded by cosmic rays. Dorman (2004) defines cosmic rays "as particles and photons with energies at least several orders of magnitude higher than the average energy of thermal particles of background plasma." Cosmic rays have different origins, there are extragalactic (up to $10^{21}$ eV), galactic (at least up to $10^{15}$–$10^{16}$ eV), and solar (with energy up to 15–30 GeV) cosmic rays (Dorman, 2004). Solar cosmic rays constitute a population of energetic charged particles ejected by the Sun during eruptive events (e.g., solar flares). Most of the solar cosmic rays are protons; thus, sometimes they are called "solar proton events" (SPEs) (e.g., Bazilevskaya et al., 2008; Desai & Giacalone, 2016; Vainio et al., 2009). Cosmic rays lose their energy throughout interactions with the atmosphere of the Earth producing secondary particles, and can then be detected by neutron monitors (NM) installed on the ground. Solar disturbances can produce cosmic ray variations detected by the NM, such as: Ground Level Enhancements (GLEs) and Forbush decreases (FD) which are sudden increases and depressions of the cosmic ray flux, respectively (Cane, 2000; Poluianov et al., 2017).

These energetic charged particles interact with the middle and lower atmosphere of the Earth. One mechanism by which they deposit their energy is by ionization, by modifying atmospheric chemistry. This topic has been studied for a long time and it remains important in the relationship between space weather and tropospheric climate. However, the involved mechanisms are not well understood. Although the influence of solar variability in the lowest atmosphere is probably weak, the coupling between space weather and the tropospheric climate has been recognized as potentially important for the human environment (Gray et al., 2010; Lilensten et al., 2016). This coupling could exist through the Global Electric Circuit, the GEC (Rycroft et al., 2012). Previous works have shown various short-term effects of SPE and FD events on the GEC parameters (Golubenko et al., 2020; Mironova et al., 2015). For example, balloon measurements recorded at ∼30 km showed an increase of the electrical conductivity and decrease of the atmospheric electric field, in fair weather conditions, after the occurrence of intense SPEs (Holzworth & Mozer, 1979; Holzworth et al., 1987; Kokorowski et al., 2006; Reagan et al., 1983). These variations were caused by ionization in the lower atmosphere. Furthermore, SPE effects were also observed in the atmospheric electric field variation recorded at ground levels in fair weather regions (Cobb, 1967; Elhalel et al., 2014; Märcz, 1987; Nicoll & Harrison, 2014; Reiter, 1969, 1971; Sartor, 1980; Sheftel et al., 1994; Takagi & Iwata, 1984). However, a correct choice for isolated SPEs was not performed, meaning that during the SPEs onset, other solar disturbances may have happened simultaneously (e.g., geomagnetic disturbances or FDs). Tacza et al. (2018) performed the analysis of 15 SPEs clearly isolated from the occurrence of geomagnetic storms or FDs. The authors found an average increase of ∼13% of the atmospheric electric field after the SPE onset, when compared with mean values. The explanation of the atmospheric electric field increase due to SPEs can be based on the model of Farrell and Desch (2002), which proposed that SPEs increase the electrical conductivity above the "batteries" (thunderstorms and electrified shower clouds) of the GEC, reducing the ohmic resistance above them, and allowing more current to flow upward. This produces an increase of the atmospheric electric field in fair weather regions. Recently, Wu et al. (2020) found an increase in the lightning density after very intense SPEs, which brings new insights in that SPEs not only changes the electrical conductivity above the "batteries" of the GEC, but also could influence the "batteries."

Additionally, the impact of FDs in the GEC parameters has been reported (Engfer & Tinsley, 1999; Märcz, 1997; Okike & Umahi, 2019; Okike, 2019; Sheftel et al., 1994). Sheftel et al. (1994) used several midlatitude stations and found an immediate increase of the current density following the onset of six Forbush decrease events. Okike and Umahi (2019) found a reduction in the lightning occurrence on a global scale during the FD onset. Furthermore, Okike (2019) reported that lightning occurrences reduction during FDs showed significant correlations at the United States latitude band and within the African region. In fair weather conditions, Märcz (1997) found a decrease of the atmospheric electric field, after FD events recorded at Nagycenk observatory (Hungary). However, Engfer and Tinsley (1999) found no significant variation in the atmospheric electric field, after FDs recorded at Mauna Loa (Hawaii).

In this context, there is clearly a need for more observational studies to assess the impact of energetic charged particles during SPEs and the effects of FDs on the GEC. The aim of this paper is to study the potential gradient diurnal curve variations observed in fair weather conditions during two types of events (a) solar proton events (SPEs) and (b) Forbush decreases (FDs). We use potential gradient data recorded between January 2010 and December 2019 at two stations at different latitudes in both hemispheres and at different altitudes: the high-altitude Complejo Astronómico El Leoncito and the lowland Swider Geophysical Observatory. In Section 2, the observation sites and instrumentation are described. The methodology and results are presented in Sections 3 and 4, respectively. Finally, we discuss and summarize our results in the last section.

## 2. Observation Site and Instrumentation

We focus on potential gradient (PG) measurements recorded in the Complejo Astronómico El Leoncito, CASLEO (31.798°S, 69.295°W, magnetic latitude 21.95°S, and altitude 2,550 m a.s.l.), located in the Argentinian Andes, and in the Świder Geophysical Observatory (52.12°N, 21.23°E, magnetic latitude 50.28°N, and altitude 100 m a.s.l.), located in Poland, during the period between January 2010 and December 2019. A detailed description of the site locations and the instrumentation are described in previous works (Kubicki et al., 2016; Tacza et al., 2021) and we only provide a brief description here.

CASLEO observatory is an astronomical observatory located in "El Leoncito," an area characterized with more than 250 clear-sky days per year, no clouds, almost no wind blowing, and a typically diaphanous, contamination-free atmosphere. The nearest town, Barreal, is located 40 km away. The PG measurements are recorded by a BOLTEK field mill sensor (PG = −Ez, where Ez is the vertical atmospheric electric field). The sensor is mounted on steel support 0.4 m above the surface. The PG values have been reduced to the value at free flat area at ground level and 1 s averages of the PG are processed. The fair-weather conditions refer to weather conditions of none or small cloudiness, no precipitation, fog or dust, and strong wind at the measurement site (e.g., Imyanitov & Chubarina, 1967). In a previous work, Tacza et al. (2021) highlighted the possibility of providing reliable PG diurnal variations in fair weather conditions at CASLEO. To ensure fulfillment of the criteria of fair-weather at CASLEO we have used a Cloud Sensor II (Boltwood Systems Corporation), and a Vantage Pro (Davis Instruments) for controlling cloudiness and the other meteorological parameters: presence of precipitation, wind speed (<6 m/s), relative humidity (<90%). Harrison and Nicoll (2018) have proposed a condition for the relative humidity <95% (and visibility of 2–5 km or greater) to fulfill the criterion of lack of hydrometeors using automated measurements.

The Stanislaw Kalinowski Geophysical Observatory in Świder is located 25 km South-Southeast of Warsaw city, and 2.5 km North-Northwest of the Otwock town. Nowadays it works mainly as an atmospheric electricity observation station. The Observatory is surrounded by pine and deciduous trees. Long term analysis of meteorological elements at Świder shows the annual mean cloudiness is 4/8. Weak winds (<2 m/s) dominate within a year, while strong winds (>6 m/s) occur during spring. At Świder station, rural continental aerosols of natural origin prevail, with an influence of anthropogenic pollution especially during winter months. We use potential gradient measurements recorded by a radioactive collector type of the electric sensor. The collector at Świder is mounted 2.0 m above the surface. All measured values have been reduced to the value at free flat area at ground level and 1 min averages of the PG are processed. At Świder the following criteria of fair weather for atmospheric electricity are used: wind speed <6 m/s, the cover of low-level clouds <4 in okta scale (4/8), no precipitation or fog, and no local or distant thunderstorms at the measurement site. These are monitored by continuous meteorological observations at the station (e.g., Kubicki et al., 2016).

## 3. Methodology

We analyze the PG diurnal variation, in fair weather conditions, during two different types of events:

1. Intense SPE, with significant proton flux above 100 MeV as detected by GOES particle instruments, and
2. Intense FD, selected by the IZMIRAN catalog (MagnM>4). MagnM indicates the FD magnitude for particles with 10 GV rigidity, corrected on magnetospheric effect with Dst-index.

For case (1), in order to get rid of the effects of other solar and/or geomagnetic disturbances, we chose SPE events such as the Kp index remained lower than 4 (Kp < 4) during three consecutive days, that is, 1 day before, and 2 days after the events. Similarly, we disregard SPE events for which an FD occurred during this three-day period. For case (2), we verify that no SPE occurred during the FD period. The list of SPE and FD events are listed in Appendices A and B, respectively. Finally, in both cases (1) and (2), during the three-day period around the event, PG hourly values that did not meet fair weather conditions were removed as defined in Section 2.

The methodology adopted in the analysis is as follows: first, monthly mean curves of the PG diurnal variation, in fair weather conditions, were calculated for each month (referred to as monthly standard curves). Second, for each SPE event (case 1), a time window of 24 hr before and 48 hr after the start time of the event is used, where the start time of the SPE is defined as the beginning of the ≥100 MeV proton flux enhancement at the GOES satellite. On the other hand, for FD events (case 2) a time window of 170 hr before and after the start time was chosen, where the start time is defined as the beginning of the FD decrease observed in three Neutron Monitor stations (Oulu-Finland, Mexico and Lomnický štít-Slovakia NM have been used). Next, in every time window, the differences between the PG hourly values and their monthly standard curves were calculated to get the PG excesses, that is, the calculated deviation of the PG from the mean value, further referred to in the text as PG deviation. Finally, the superposed epoch analysis (SEA) is applied to the PG deviation.

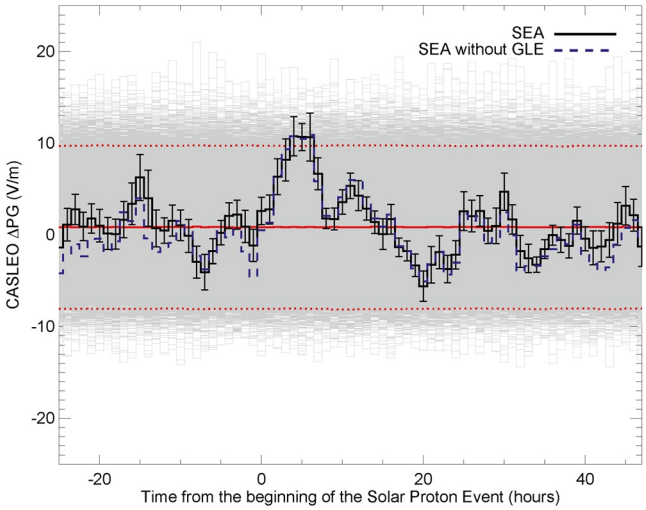


**Figure 1.** Superposed epoch analysis (SEA) of the potential gradient Complejo Astronómico El Leoncito (CASLEO) deviation response to Solar Proton Event (SPE) (black curve). The error bars represent one standard error of the mean. The gray lines show the result of 30,000 iterations doing the average of the 17 events for random starting times. The solid red line is the average of the iterations and the dashed red lines represent ±2.5 σ (σ is the standard deviation). The blue dashed line is the SEA result without considering the two Ground Level Enhancement (GLE) events.

## 4. Results

In this section we present the behavior of the potential gradient recorded at CASLEO (PG CASLEO) and SWIDER (PG SWIDER), during Solar Proton Events (SPE) and Forbush Decreases (FD). The following two subsections show the results for SPEs and FDs, respectively.

### 4.1. Potential Gradient Response to Solar Proton Events

Figure 1 shows the result of the superposed epoch analysis applied to the PG CASLEO deviations (black line) during seventeen (17) SPEs, where the time zero represents the start of the SPE. Features of each SPE are described in Appendix A (15 events were previously analyzed in Tacza et al. (2018) in connection with the PG at CASLEO–these are recalculated at present taking into account more rigorous monitoring of fair weather conditions for the PG values selection). The error bars represent one standard error of the mean. Two events were strong enough to produce Ground Level Enhancement (GLE): the SPE of 2012, May 17 (GLE71; https://gle.oulu.fi) and 2017, September 10 (GLE72). The blue dashed line is the result of the superposed epoch analysis (SEA) without considering these two GLEs. Each gray line is the result of the superposed epoch analysis choosing random starting times for the 17 SPEs (30,000 iterations). The solid red line is the average of the iterations, and the dashed red lines are ±2.5 σ (σ is the standard deviation) of the average (99% confidence level). A clear increase of ∼11 V/m in the PG CASLEO is observed after the start of the SPEs. This increase corresponds to an excess of ∼13% with respect to PG mean fair weather values.

Figure 2 shows the scatter between PG CASLEO hourly deviations and solar proton particle flux (N, units of protons. cm-2s-1sr-1), with energies >100 MeV. For this particular case, the time window only corresponds to the day of the onset of the SPE until its return to background levels, for each of the 17 events (∼479 hr). The color

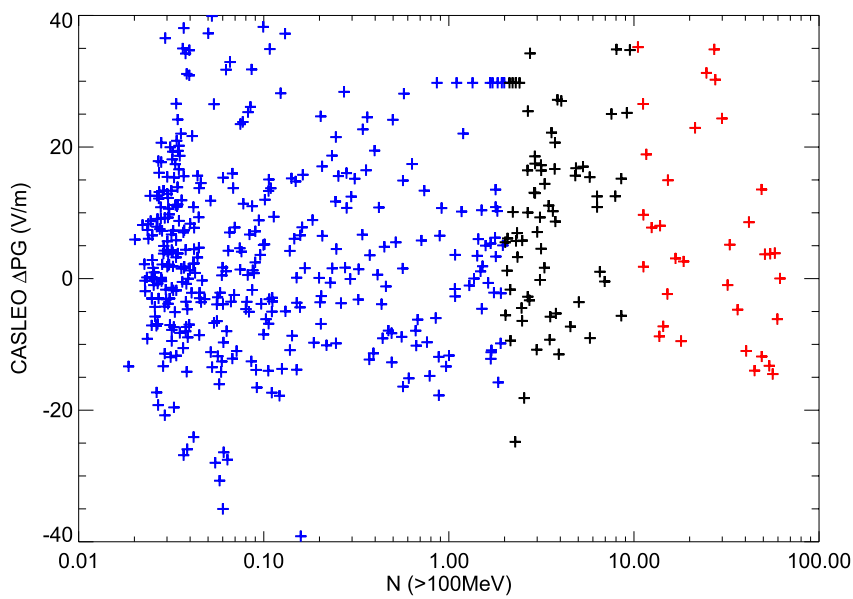


**Figure 2.** Potential gradient (PG) Complejo Astronómico El Leoncito (CASLEO) hourly deviations against *N* (psrotons/[cm$^2$ s sr]) for proton flux with energy >100 MeV, during the day of the Solar Proto Event for each of the 17 events. The colors are separated for N ranges: blue ($N$ = [0, 2]), black ($N$ = [2, 10]), and red ($N$ > 10).

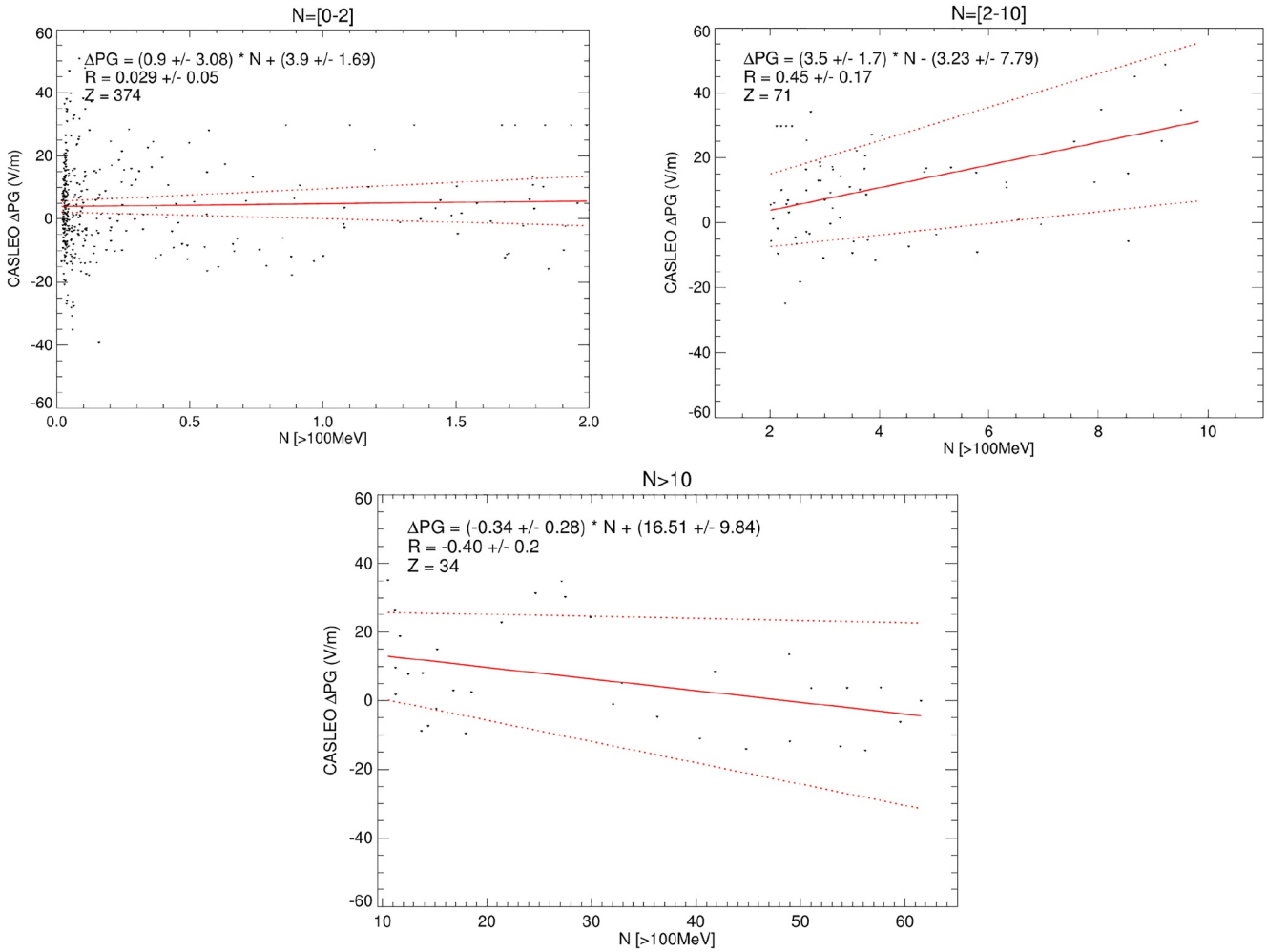


**Figure 3.** Linear regression between Potential gradient (PG) Complejo Astronómico El Leoncito (CASLEO) hourly deviation and $N$ (protons/[cm$^2$ s sr]) for energy >100 MeV, for $N$ ranges of [0–2], [2–10], and $N > 10$. Here, $R$ indicates the Pearson correlation coefficient and $Z$ is the number of points. Each parameter in the equation (slope and coefficient) and the correlation coefficient indicate the 95% confidence interval. Red dotted lines indicate the 95% confidence interval.

indicates N ranges: $N = [0, 2]$ (blue), $N = [2, 10]$ (black), and $N > 10$ (red). Figure 3 shows the linear regression between PG CASLEO hourly deviations and N (protons.cm-2s-1sr-1), separated for each N range. For N between 0 and 2: $N = [0, 2]$ the Pearson correlation coefficient ($R$) is almost zero. For N between [2, 10], a positive correlation was found ($R = 0.45$) and for $N > 10$, we note a negative correlation ($R = -0.4$). The SPE events with $N > 10$ correspond to the two GLE events: GLE71 and GLE72.

As we have done for PG CASLEO, Figure 4 shows the result of the superposed epoch analysis applied to the PG SWIDER deviations (black line). Eight (8) SPEs have been analyzed. The error bars represent one standard error of the mean. As in Figure 1, each gray line is the result of applying the superposed epoch analysis using random starting times for the SPE events (30,000 iterations). The solid red line is the average of the iterations and the dashed red lines are ±2.5 σ of the average. We do not observe any significant PG deviation after the start of SPEs.

### 4.2. Potential Gradient Response to Forbush Decreases

Figures 5 and 6 show the results of the SEA applied to the PG CASLEO and PG SWIDER deviations (black line in both cases), respectively, during FD events. As we have done before for SPEs, the time zero represents

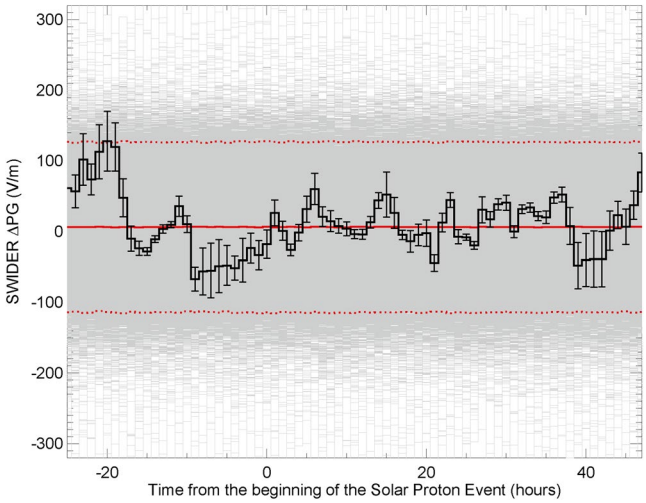


**Figure 4.** As described for Figure 1 but for the Potential gradient (PG) Geophysical Observatory in Świder (SWIDER) data (eight events).

the starting time of the FD. The figures illustrate 18 events for CASLEO and 15 events for SWIDER, since the number of detected events at a given place depends on fair-weather conditions. Features of the FDs are described in Appendix B. The error bars represent one standard error of the mean. Each gray line is the result of the superposed epoch analysis choosing FDs random starting times (30,000 iterations). The solid red line is the average of the iterations, and the dashed red lines are ±2.5 σ of the average (99% confidence level). No significant PG deviation is observed.

Figures 7, 8, and 9, show individual analysis for three very pronounced FDs that occurred during: 21–27 of June 2015 (MagnM > 10.4%), 12–18 of July 2012 (MagnM > 8.2%), and 15–21 of July 2017 (MagnM > 6.7%), respectively. Each figure shows the diurnal variation of the Dst index (black curve) and Kp index (red curve) in the first panel from the top. Second panel show the relative (to the mean average) variation of the cosmic ray fluxes detected in three neutron monitor stations: Oulu (blue curve), Lomnický štít-Slovakia (LMKS; Slovakia, red curve), and MXCO (Mexico, black curve). In these figures, Rc indicates the geomagnetic rigidity cutoff in each station. Additionally, the solar proton fluxes above 100 MeV (green curve) are plotted. The third panel from the top show the cosmic ray flux in counts per 500 milliseconds detected by the CARPET monitor (installed at CASLEO, Rc = 9.8 GV). The PG CASLEO diurnal variation and the PG CASLEO monthly standard curve is shown in the fourth panel (black curve and gray curve, respectively). The error bar indicates ± 1 σ. Bottom panel show the PG CASLEO deviation. In Figures 7 and 8, the PG SWIDER deviation is also shown (red curve) in the bottom panels. Gaps in the PG variation indicate the absence of fair-weather conditions and these PG values were removed, as explained in the methodology section.

The FD that occurred between 21 and 27 of June 2015 (Figure 7), was associated with an intense geomagnetic storm, where the Dst index reached its minimum on June 23rd at ∼4UT (Dst = −200 nT, Kp = 8). A similar temporal behavior is observed when comparing the cosmic ray flux detected in the three neutron monitors and the CARPET detector, all showing two pronounced minima. The first minimum occurred at the same time as the minimum in the Dst index, and the second minimum was observed on June 25th at ∼0UT. There is a large variability observed in the PG CASLEO values, around ±30%, but there is a sustainable increase of the PG CASLEO values specially for June 23rd, which coincides in time with the first minimum on the cosmic ray flux and the minimum in the Dst index. No significant change of the PG CASLEO values is observed during the second minimum. For PG SWIDER, most of the first pronounced minimum on June 23rd was outside fair weather conditions, and no significant variation is observed during the second minimum.

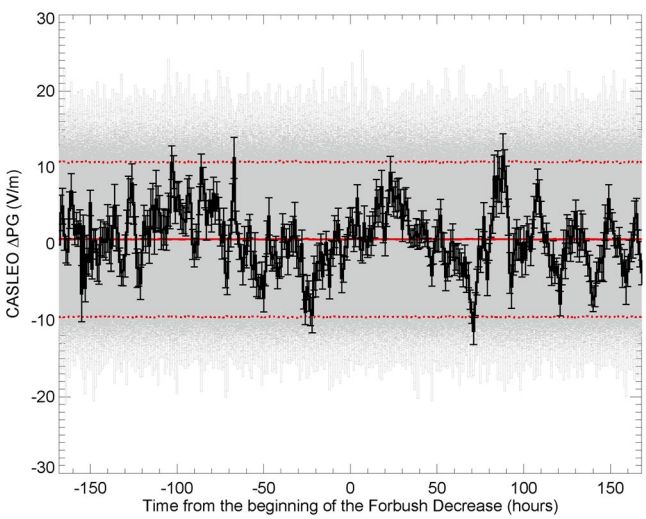


**Figure 5.** Superposed epoch analysis of the Potential gradient (PG) Complejo Astronómico El Leoncito (CASLEO) deviation response to Forbush Decrease (black curve). The gray lines show the result of 30,000 iterations doing the average of the 18 events in different times. The solid red line is the average of the iterations and the dashed red lines represent ±2.5 σ.

The FD that occurred between 12 and 18 of July 2012 (Figure 8) was also associated with an intense geomagnetic storm, where the Dst index reached its minimum on July 15th at ∼16UT (Dst = −139 nT, Kp = 7). There is a broad minimum observed in the NM during 15 and 16 of July and for the CARPET detector there is a clear minimum at the end of July 15th and start of July 16th. A clear increase is detected in the PG CASLEO values, which occurred at the same time of the minimum observed in the CARPET data. Nonsignificant variation in the PG SWIDER values was observed.

On the other hand, the FD that occurred between 15 and 21 July 2017 (Figure 9) was associated with a moderate geomagnetic storm, where the Dst index reached its minimum on July 16th at ∼15UT (Dst = −72 nT, Kp = 5). A minimum occurs at the end of July 16th which is detected in

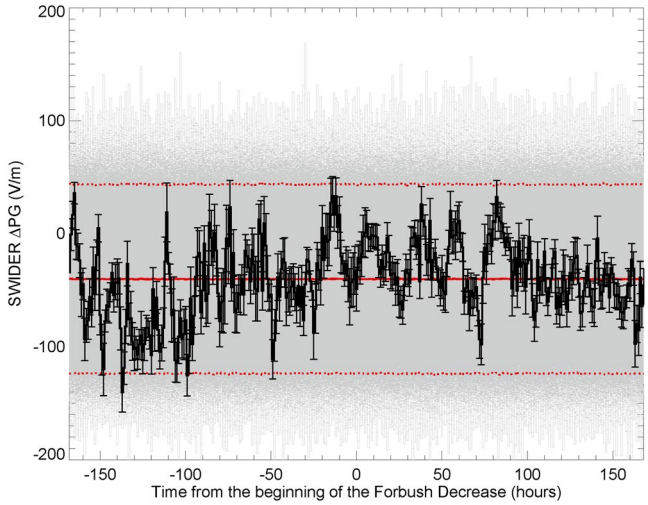


**Figure 6.** As described for Figure 5 but for the Potential gradient (PG) Geophysical Observatory in Świder data (15 events).

the three NM stations. Interestingly, the minimum in the CARPET detector is more pronounced at the start of July 17th. There is a clear increase of the PG CASLEO values at the time of the cosmic ray flux minima detected by NMs.

## 5. Discussions and Summary

In this article, we present the PG variations during very intense Solar Proton Events (SPE), case 1, and Forbush Decrease (FD) events, case 2. The analysis was performed for PG, at fair weather conditions, recorded at two stations located in low and middle (magnetic) latitudes, and at two different altitudes: CASLEO (low latitude, 2550 m a.s.l.) and SWIDER (middle latitude, 100 m a.s.l.). We applied the superposed epoch analysis in order to enhance some possible weak effects and remove the noise produced by meteorological parameters.

For case 1, the results obtained show an increase of the PG values (∼11 V/m) after the SPE recorded at CASLEO station (Figure 1), which represents an increase of ∼13% with respect to the PG mean values. It is noted that the PG increase is greater than the background variability (±6 V/m). Furthermore, Figure 3 indicates that the increase is directly related with the solar proton flux particles (N). When $N = [0, 2]$ there are not any changes in the PG (Pearson correlation coefficient, $R \sim 0$), but when $N = [2, 10]$ a positive correlation was found with the PG (with $R \sim 0.45$). PG increases associated with SPEs have been reported by other authors (e.g., Cobb, 1967; Reiter, 1971). Although it is very unlikely that SPE itself can reach the ground level (except GLEs), they can reach stratospheric altitudes in the polar and middle-latitude atmosphere, as well as cause changes in the chemistry of the layer (Bazilevskaya et al., 2010; Sinnhuber et al., 2012). Nevertheless, Nicoll and Harrison (2014) reported an increase of the atmospheric ionization in the lower atmosphere (between 10 and 25 km) recorded at a midlatitude site (51.45°N). This increase indicates penetration of energetic particles well into the troposphere during the SPE that occurred on 11 April 2013 (not cataloged as GLE).

Farrell and Desch (2002) suggested one mechanism about how SPE produces an increase of the potential gradient in fair weather regions. The authors proposed that SPEs can increase the electrical conductivity above thunderstorms allowing more current flows in the global electric circuit, and thus, producing an increase in the potential gradient in fair weather conditions recorded at the ground level. Similar mechanism was proposed previously by Markson (1978) and Willet (1979). It is known that main thunderstorms regions are in the tropical zone (Christian et al., 2003). However, thunderstorms at midlatitudes, specifically in the Northern Hemisphere, are not insignificant (Christian et al., 2003). This is confirmed by recent studies (Blakeslee et al., 2020; Kaplan & Lau, 2021). Furthermore, Holzworth et al. (2021) reported an increase of lightning above 65°N since 2012. Taking into account that thunderstorms occurrence above midlatitudes is significant, the mechanism suggested by Farrell and Desch (2002) is plausible.

On the other hand, for $N > 10$, a negative correlation was found ($R \sim -0.4$). Only two SPEs events contributed to this analysis and, moreover, these SPEs were strong enough to reach the ground level. These events were cataloged as Ground Level Enhancements (GLE 71 and GLE72). In Tacza et al. (2018), the authors showed in detail the PG analysis during GLE71, discarding any meteorological or geomagnetic effects. The authors suggested that GLE71 increased the electrical conductivity at the ground level and, by Ohm's law, this produced a decrease of the PG. This seems also to be the case for GLE72, when any meteorological or geomagnetic effects were also discarded. Nevertheless, analysis of more GLE events is necessary to evaluate and support our hypothesis.

However, no significant changes in the PG at SWIDER station during SPEs were found. One reason for the lack of effects could be the very few events included in the analysis (8 events). SWIDER PG data show high variability of the background level (±80 V/m) and it can hide any statistically significant SPE effect. Although

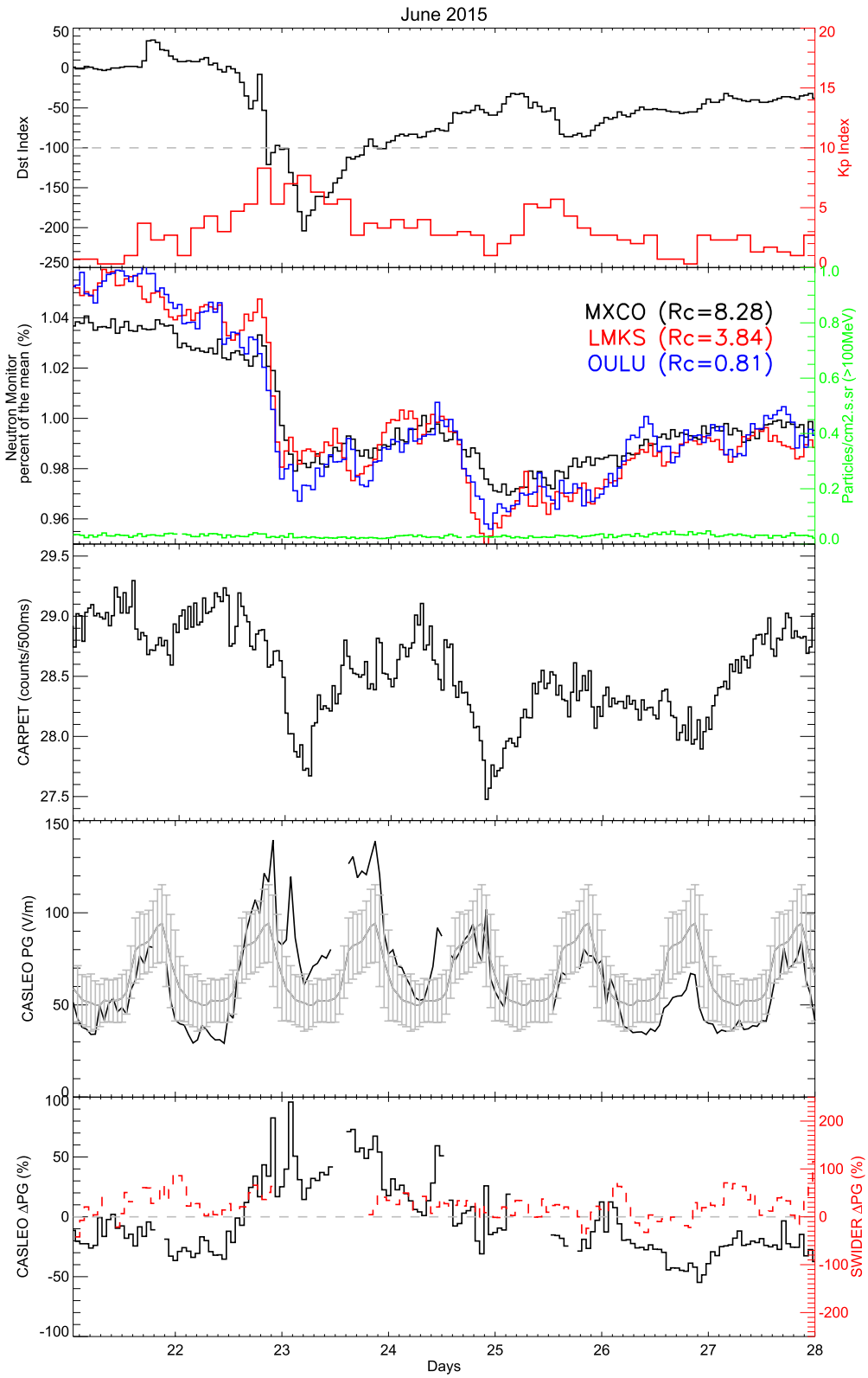
June 2015
Dst Index
Kp Index
MXCO (Rc=8.28)
LMKS (Rc=3.84)
OULU (Rc=0.81)
Neutron Monitor percent of the mean (%)
Particles/cm2.s.sr (>100MeV)
CARPET (counts/500ms)
CASLEO PG (V/m)
CASLEO ΔPG (%)
SWIDER ΔPG (%)
Days

**Figure 7.**

SPEs effects in the PG variation have mostly been reported at locations remote from cities and elevated regions, such as mountains (Cobb, 1967; Reiter, 1971; Tacza et al., 2018), there are also reports of SPE effects on the PG close to urban sites (e.g., Nicoll & Harrison, 2014). However, the air pollution at urban sites is a problem, since the attachment of aerosol particles to atmospheric ions reduces the conductivity producing an increase in the PG values (Kubicki et al., 2016). An analysis of more SPEs at other locations and altitudes can cast light on this issue.

For case 2, no significant PG variation was found at CASLEO and SWIDER stations after the FD onset (Figures 5 and 6, respectively). It is worth mentioning that we chose FD with MagnM > 4 (according to the IZMIRAN database). We selected 18 events for CASLEO and 15 events for SWIDER, among which 6 and 8 events were greater than MagnM > 6 for CASLEO and SWIDER, respectively. In a previous work, Engfer and Tinsley (1999) studied PG variation recorded at Mauna Loa (3,400 m a.s.l.) in association with FD events. The authors analyzed 93 FDs and did not find any significant PG variation. Additionally, Märcz (1997) reported the PG variations recorded at Nagycenk Observatory (Hungary, altitude: 154 m a.s.l.) during 60 FD events. The author found a PG decrease during the following 2–4 days after the FD onset. However, as reported by the author, this result is in contrast with some models which argue that intense FD events produce a decrease of the electrical conductivity profile, which increases the potential gradient and the air-Earth current at ground level (e.g., Makino & Ogawa, 1984). In earlier studies Märcz (1987) discovered an increase of SWIDER PG on the sixth day after intense solar flares compared to the monthly level which the author related to after-effects in the ionospheric absorption.

In our study, individual analysis of the three larger FD events that occurred during 21–27 June 2015 (MagnM = 10.4), 12–18 July 2012 (MagnM = 8.2), and 15–21 July 2017 (MagnM = 6.7), showed an increase of the PG values at CASLEO (Figures 7, 8, and 9, respectively). It agrees with the models reported. Additionally, a decrease of the cosmic ray flux at CASLEO station was also observed, supporting the general idea that the electrical conductivity profile might also have decreased. On the other hand, there was no significant variation for PG SWIDER values (Figures 7 and 8). To this respect, it is worth mentioning that the PG SWIDER values did not meet fair weather conditions (values were removed) during most part of the minimum observed in the cosmic rays. The results observed at CASLEO suggest that only very intense FD events can produce PG variation measured at ground level, and this can be a reason why it was not observed using the superposed epoch analysis (many events with MagnM < 6).

This paper reports results of study of the effects of energetic particles (Solar Proton Events) and Forbush decreases on the potential gradient variation in more detail by looking at simultaneous variations recorded at two stations located at low (CASLEO) and mid (SWIDER) magnetic latitudes and at different altitudes. In summary, our results confirm SPEs influence on the PG variation recorded at ground level at a clean and high-altitude site, similar in nature to those observed by Cobb (1967) at Mauna Loa and Reiter (1969) at Zugspitze, and in the initial investigation at CASLEO (Tacza et al., 2018). Our findings support the suggestions that SPE effects are observed only at high-altitude sites (Märcz, 1987; Reiter, 1971). On the other hand highly energetic charged particle effects, such as Ground Level Enhancement, and phenomena as Forbush decreases, can modulate the electrical conductivity profile producing local changes in the PG at the ground level such as observed by Märcz (1997) at Nagycenk or Kleimenova et al. (2009) at Swider for selected cases. Such an effect also emerges at CASLEO during GLE events 71 and 72. Our work is still ongoing, and future studies will focus on analysis of a larger data set of different stations worldwide.

**Figure 7.** (first panel) Dst index (black curve) and Kp index (red curve) hourly variation for the period between 21 and 27 June 2015. (second panel) Neutron monitor count rate enhancements at Mexico (black curve), LMKS (red curve), and Oulu (blue curve) stations. The energetic protons flux in the channel ≥100 MeV (green curve) is also shown. (third panel) Cosmic ray counting ray in the detector CARPET. (fourth panel) Complejo Astronómico El Leoncito (CASLEO) Potential gradient (PG) hourly values for the day of the event (black curve) and the monthly standard curve (gray curve) with their respective error bars of ±1 standard deviation (±1 σ). (fifth panel) PG deviations for CASLEO (black curve) and Geophysical Observatory in Świder (SWIDER; red curve) stations. Gaps in the PG values are due to not meeting fair weather conditions.

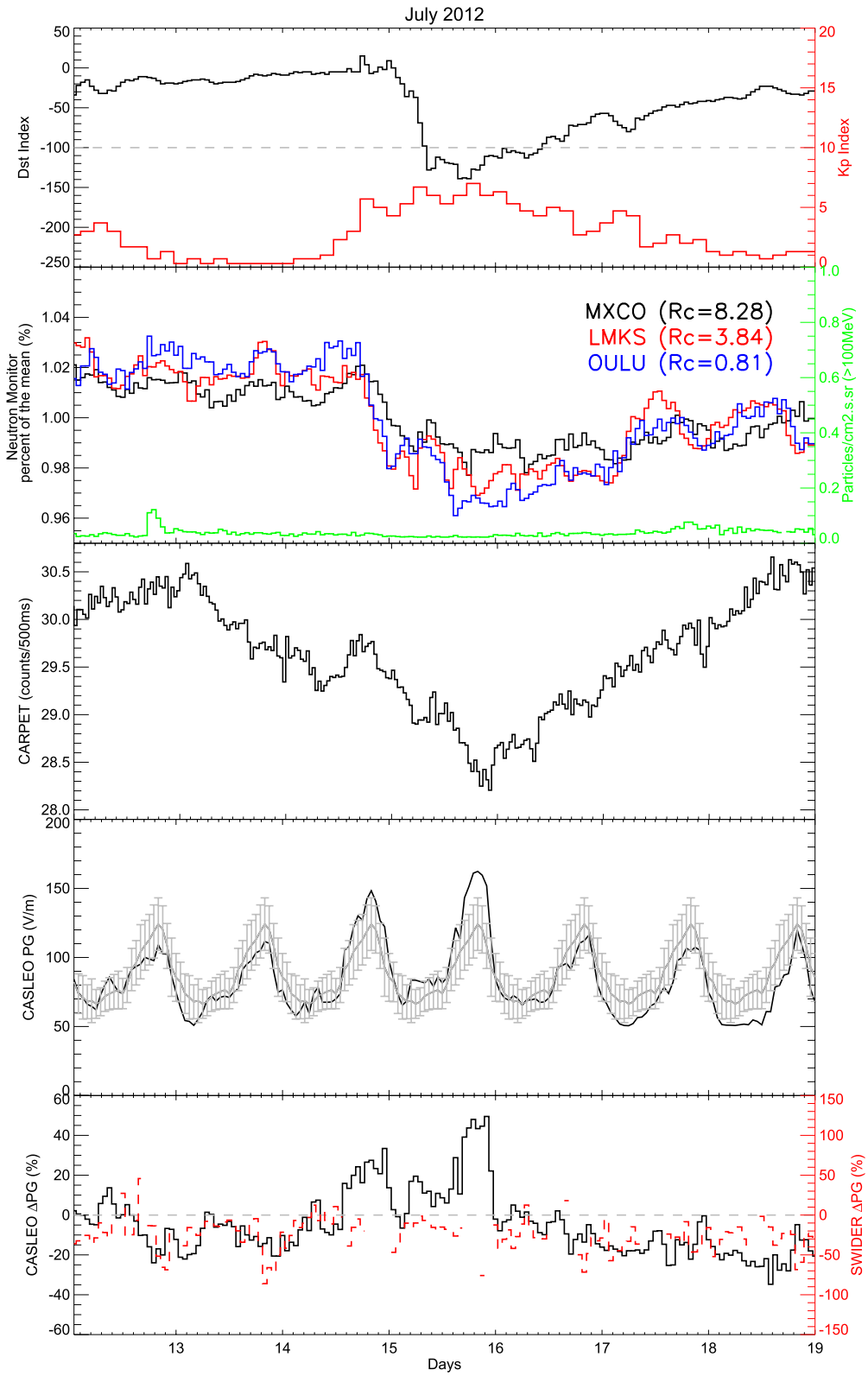


**Figure 8.** As described for Figure 7 but for the period between 12 and 18 July 2012.

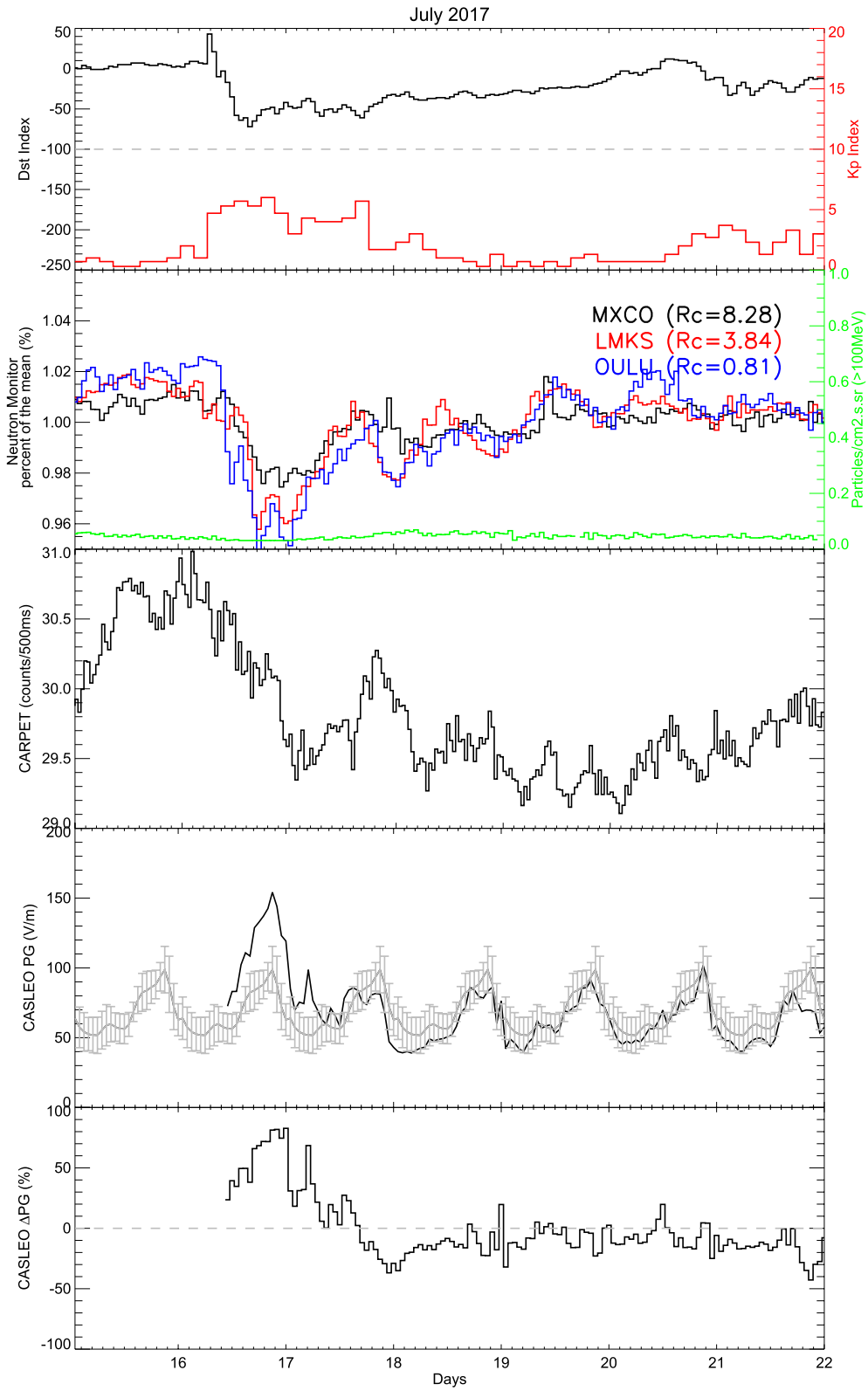


**Figure 9.** As described for Figure 7 but for the period between 15 and 21 July 2017.

## Appendix A: Solar Proton Event List

Table A1 lists the solar proton events chose according to the criteria described in Section 2. The information was obtained from ftp://ftp.swpc.noaa.gov/pub/indices/SPE.txt and ftp://ftp.swpc.noaa.gov/pub/warehouse. The two events classified as Ground Level Enhancement (GLE) were 17 May 2012 (GLE 71) and 10 September 2017 (GLE 72) (https://gle.oulu.fi/#/).

**Table A1**
*List of the Solar Proton Events Chosen for Our Analysis*

| N° | Date | Start (UT) | Particles (MeV) | Proton fluence (protons/cm$^2$daysr) | PG station where FW was accomplished |
|---|---|---|---|---|---|
| 1 | 2011/03/21 | 4 | ≥100 | 8.4e + 03 | CASLEO/SWIDER |
| 3 | 2011/09/06 | 23 | ≥100 | 5.0e + 03 | SWIDER |
| 4 | 2011/09/23 | 2 | ≥100 | 7.7e + 03 | CASLEO |
| 5 | 2012/01/27 | 18 | ≥100 | 1.6e + 05 | CASLEO/SWIDER |
| 6 | 2012/05/17 | 2 | ≥100 | 3.2e + 05 | CASLEO |
| 7 | 2012/07/12 | 17 | ≥100 | 3.7e + 03 | CASLEO |
| 8 | 2012/07/19 | 7 | ≥100 | 1.9e + 04 | CASLEO |
| 9 | 2012/07/23 | 7 | ≥100 | 2.9e + 04 | SWIDER |
| 10 | 2012/09/28 | 1 | ≥100 | 5.0e + 03 | CASLEO |
| 11 | 2013/04/11 | 8 | ≥100 | 7.0e + 04 | CASLEO |
| 12 | 2013/05/15 | 12 | ≥100 | 2.8e + 03 | CASLEO/SWIDER |
| 13 | 2013/05/22 | 14 | ≥100 | 9.4e + 04 | CASLEO |
| 14 | 2013/09/30 | 2 | ≥100 | 6.5e + 03 | CASLEO/SWIDER |
| 15 | 2013/10/28 | 18 | ≥100 | 4.1e + 03 | SWIDER |
| 16 | 2014/01/06 | 8 | ≥100 | 9.4e + 04 | CASLEO |
| 17 | 2014/01/07 | 19 | ≥100 | 6.1e + 04 | CASLEO |
| 18 | 2014/02/20 | 8 | ≥100 | 2.2e + 03 | CASLEO |
| 19 | 2014/04/18 | 12 | ≥100 | 1.3e + 04 | CASLEO |
| 20 | 2015/10/29 | 3 | ≥100 | 4.7e + 04 | CASLEO/SWIDER |
| 21 | 2017/09/10 | 15 | ≥100 | 1.1e + 06 | CASLEO |

## Appendix B: Forbush Decrease List

Table B1 lists the Forbush decreases events chose according to the criteria described in Section 2. The information was obtained from http://spaceweather.izmiran.ru/eng/dbs.html.

**Table B1**
*List of the Forbush Decreases Events Chosen for Our Analysis*

| N° | Date–Time (YY/MM/DD–HH:MM:SS UT) | MagnM (%) | $B_{max}$ (nT) | $Bz_{min}$ (nT) | $V_{max}$ (Km/s) | $Dst_{min}$ (nT) | PG station where FW was accomplished |
|---|---|---|---|---|---|---|---|
| 1 | 2011/06/22–03:00:00 | 4.4 | 10.5 | −5.3 | 661 | −26 | CAS |
| 2 | 2011/08/05–17:51:00 | 5.1 | 29.4 | −18.7 | 611 | −115 | CAS/SWI |
| 3 | 2011/09/26–12:35:00 | 5.6 | 34.2 | −16.4 | 704 | −101 | CAS |
| 4 | 2011/10/24–18:31:00 | 6.8 | 24 | −11.6 | 516 | −147 | SWI |
| 5 | 2012/06/16–20:19:00 | 4.8 | 40.1 | −16.0 | 519 | −86 | CAS/SWI |
| 6 | 2012/07/14–18:09:00 | 8.2 | 27.3 | −17.7 | 667 | −133 | CAS/SWI |
| 7 | 2012/11/12–23:11:00 | 4.5 | 22.8 | −17.5 | 454 | −109 | CAS |

**Table B1**
*Continued*

| N° | Date–Time (YY/MM/DD–HH:MM:SS UT) | MagnM (%) | $B_{max}$ (nT) | $Bz_{min}$ (nT) | $V_{max}$ (Km/s) | $Dst_{min}$ (nT) | PG station where FW was accomplished |
|---|---|---|---|---|---|---|---|
| 8 | 2012/11/23–21:51:00 | 4.2 | 15.1 | −6.9 | 409 | −42 | CAS |
| 9 | 2013/03/17–05:59:00 | 5.0 | 17.8 | −14.0 | 725 | −132 | CAS/SWI |
| 10 | 2013/04/13–22:54:00 | 5.3 | 12.9 | −4.5 | 516 | −16 | CAS |
| 11 | 2013/06/23–04:26:00 | 6.0 | 7.6 | −5.0 | 697 | −49 | CAS |
| 12 | 2014/02/15–13:16:00 | 4.3 | 16.2 | −8.3 | 450 | −27 | SWI |
| 13 | 2014/02/27–16:50:00 | 5.5 | 16.6 | −12.7 | 483 | −99 | CAS/SWI |
| 14 | 2014/04/18–02:00:00 | 4.2 | 10.2 | −6.7 | 506 | −13 | CAS/SWI |
| 15 | 2014/06/07–16:52:00 | 4.5 | 26.0 | −8.7 | 616 | −38 | SWI |
| 16 | 2014/09/12–15:53:00 | 6.9 | 31.7 | −9.5 | 730 | −75 | SWI |
| 17 | 2014/12/21–19:11:00 | 7.0 | 16.7 | −15.5 | 429 | −51 | CAS |
| 18 | 2015/03/17–04:45:00 | 6.6 | 31.5 | −24.1 | 683 | −223 | CAS/SWI |
| 19 | 2015/06/22–18:33:00 | 10.4 | 37.7 | −26.3 | 742 | −204 | CAS/SWI |
| 20 | 2015/08/25–18:00:00 | 4.2 | 14.2 | −13.1 | 417 | −77 | SWI |
| 21 | 2015/11/06–18:18:00 | 4.0 | 19.4 | −10.3 | 677 | −96 | CAS |
| 22 | 2017/07/16–05:59:00 | 6.7 | 23.7 | −20.4 | 625 | −72 | CAS/SWI |
| 23 | 2017/09/07–23:00:00 | 9.3 | 27.3 | −23.6 | 821 | −142 | CAS/SWI |

## Data Availability Statement

CASLEO and SWIDER PG data, and CARPET data are available via: http://doi.org/10.5281/zenodo.5553010. Dst index, Kp index and solar proton flux were obtained from https://omniweb.gsfc.nasa.gov/form/dx1.html. Neutron monitor data were obtained from https://www.nmdb.eu/nest/. Forbush decreases list were obtained from http://spaceweather.izmiran.ru/eng/dbs.html. GLEs list were obtained from https://gle.oulu.fi/#/.

**Acknowledgments**
JT acknowledges the Polish National Agency for Academic Exchange for funding of the Ulam Program scholarship, agreement no PPN/ULM/2019/1/00328/U/00001. JPR thanks funding agencies CNPq (project: 310350/2019-0) and CAPES (project: 88881.310386/2018-01). AO and MK was financed with a subsidy from the Ministry of Education and Science to the Institute of Geophysics of the Polish Academy of Sciences. The authors thank the reviewers for their constructive comments and suggestions, which helped to improve the quality of the paper.

## References

Bazilevskaya, G. A., Makhmutov, V. S., Stozhkov, Y. I., Svirzhevskaya, A. K., & Svirzhevsky, N. S. (2010). Solar proton events recorded in the stratosphere during cosmic ray balloon observations in 1957–2008. *Advances in Space Research*, *45*(5), 603–613. https://doi.org/10.1016/j.asr.2009.11.009

Bazilevskaya, G. A., Usoskin, I. G., Fluckiger, E. O., Harrison, R. G., Desorgher, L., Butikofer, R., et al. (2008). Cosmic rays induced ion production in the atmosphere. *Space Science Reviews*, *137*(1–4), 149–173. https://doi.org/10.1007/s11214-008-9339-y

Blakeslee, R. J., Lang, T. J., Koshak, W. J., Buechler, D., Gatlin, P., Mach, D. M., et al. (2020). Three years of the lightning imaging sensor onboard the international space station: Expanded global coverage and enhanced application. *Journal of Geophysical Research: Atmospheres*, *125*(16), e2020JD032918. https://doi.org/10.1029/2020JD032918

Cane, H. V. (2000). Coronal Mass Ejections and Forbush decreases. *Space Science Reviews*, *93*, 55–77. https://doi.org/10.1007/978-94-017-1187-6_4

Christian, H. J., Blakeslee, R. J., Boccipio, D. J., Boeck, W. L., Buechler, D. E., Driscoll, K. T., et al. (2003). Global frequency and distribution of lightning as observed from space by the Optical Transient Detector. *Journal of Geophysical Research*, *108*(D1), 4005. https://doi.org/10.1029/2002jd002347

Cobb, W. E. (1967). Evidence of a solar influence on the atmospheric electric elements at Mauna Loa observatory. *Monthly Weather Review*, *95*(12), 905–911. https://doi.org/10.1175/1520-0493(1967)095<0905:eoasio>2.3.co;2

Desai, M., & Giacalone, J. (2016). Large gradual solar energetic particle events. *Living Reviews in Solar Physics*, *13*(1), 3. https://doi.org/10.1007/s41116-016-0002-5

Dorman, L. I. (2004). *Cosmic rays in the Earth's Atmosphere and underground. Astrophysics and Space Science Library* (Vol. 303). Kluwer Academic Publishers.

Elhalel, G., Yair, Y., Nicoll, K., Price, C., Reuveni, Y., & Harrison, R. G. (2014). Influence of short-term solar disturbances on the fair weather conduction current. *Journal of Space Weather and Space Climate*, *4*, A26. https://doi.org/10.1051/swsc/2014022

Engfer, D., & Tinsley, B. A. (1999). An investigation of short-term solar wind modulation of atmospheric electricity at Mauna Loa Observatory. *Journal of Atmospheric and Solar-Terrestrial Physics*, *61*(13), 943–953. https://doi.org/10.1016/s1364-6826(99)00057-7

Farrell, W. M., & Desch, M. D. (2002). Solar proton events and the fair weather field at ground. *Geophysical Research Letters*, *29*(9), 1323. https://doi.org/10.1007/s11214-012-9923-z

Golubenko, K., Rozanov, E., Mironova, I., Karagodin, A., & Usoskin, I. (2020). Natural sources of ionization and their impact on atmospheric electricity. *Geophysical Research Letters*, *47*(12), e2020GL088619. https://doi.org/10.1029/2020gl088619

Gray, L. J., Beer, J., Geller, J., Haigh, J. D., Lockwood, M., Matthes, K., et al. (2010). Solar influences on climate. *Reviews of Geophysics*, *48*(4), RG4001. https://doi.org/10.1029/2009rg000282

Harrison, R. G., & Nicoll, K. A. (2018). Fair weather criteria for atmospheric electricity measurements. *Journal of Atmospheric and Solar-Terrestrial Physics*, *179*, 239–250. https://doi.org/10.1016/j.jastp.2018.07.008

Holzworth, R., & Mozer, F. S. (1979). Direct evidence of solar flare modification of stratospheric electric field. *Journal of Geophysical Research*, *84*(A6), 2559–2566. https://doi.org/10.1029/ja084ia06p02559

Holzworth, R. H., Brundell, J. B., McCarthy, M. P., Jacobson, A. R., Rodger, C. J., & Anderson, T. S. (2021). Lightning in the Arctic. *Geophysical Research Letters*, *48*(7), e2020GL091366. https://doi.org/10.1029/2020gl091366

Holzworth, R. H., Norville, K. W., & Williamson, P. R. (1987). Solar flares perturbations in stratospheric current systems. *Geophysical Research Letters*, *14*(8), 852–855. https://doi.org/10.1029/gl014i008p00852

Imyanitov, I. M., & Chubarina, Y. V. (1967). *Electricity of free atmosphere, technical translation from Russian*. NASA. F-425.

Kaplan, J. O., & Lau, K. H. (2021). The WGLC global gridded lightning climatology and time series. *Earth System Science Data*, *13*(7), 3219–3237. https://doi.org/10.5194/essd-13-3219-2021

Kleimenova, N., Kozyreva, O., Kubicki, M., & Michnowski, S. (2009). Variations of mid-latitude atmospheric electric field (Ez) associated with geomagnetic disturbances and Forbush decreases of cosmic rays. *Publications of the Institute of Geophysics, Polish Academy of Sciences*, *412*(D-73), 55–64.

Kokorowski, M., Sample, J. G., Holzworth, R. H., Bering, E. A., Bale, S. D., Blake, J. B., et al. (2006). Rapid fluctuations of stratospheric electric field following a solar energetic particle event. *Geophysical Research Letters*, *33*(20), L20105. https://doi.org/10.1029/2006gl027718

Kubicki, M., Odzimek, A., & Neska, M. (2016). Relationship of ground-level aerosol concentration and atmospheric electric field at three observation sites in the Arctic, Antarctic and Europe. *Atmospheric Research*, *178–179*, 329–346. https://doi.org/10.1016/j.atmosres.2016.03.029

Lilensten, J., Dudok de Wit, T., & Matthes, K. (2016). *Earth's climate response to a Changing Sun*. EDP Sciences.

Makino, M., & Ogawa, T. (1984). Responses of atmospheric electric field and air-earth current to variation of conductivity profiles. *Journal of Atmospheric and Solar-Terrestrial Physics*, *46*(5), 431–445. https://doi.org/10.1016/0021-9169(84)90087-4

Märcz, F. (1987). *Atmospheric electric potential gradient following selected solar flare events* (Vol. 198, D-26, pp. 85–96). Publications of the Institute of Geophysics, Polish Academy of Sciences.

Märcz, F. (1997). Short-term changes in atmospheric electricity associated with Forbush decreases. *Journal of Atmospheric and Solar-Terrestrial Physics*, *59*(9), 975–982. https://doi.org/10.1016/s1364-6826(96)00076-4

Markson, R. (1978). Solar modulation of atmospheric electrification and possible implications for the Sun-weather relationship. *Nature*, *273*(5658), 103–109. https://doi.org/10.1038/273103a0

Mironova, I. A., Aplin, K. A., Arnold, F., Bazilevskaya, G. A., Harrison, R. G., Krivolutsky, A. A., et al. (2015). Energetic particle influence on the Earth's Atmosphere. *Space Science Reviews*, *194*(1–4), 1–96. https://doi.org/10.1007/s11214-015-0185-4

Nicoll, K. A., & Harrison, R. G. (2014). Detection of lower tropospheric responses to solar energetic particles at midlatitudes. *Physical Review Letters*, *112*(221–5), 225001. https://doi.org/10.1103/physrevlett.112.225001

Okike, O. (2019). Investigation of Forbush Decreases and other solar/geophysical agents associated with lightning over the U.S. latitude band and the continental Africa. *Journal of Geophysical Research: Space Physics*, *124*(6), 3910–3925. https://doi.org/10.1029/2018ja026456

Okike, O., & Umahi, A. E. (2019). Cosmic ray-global lightning causality. *Journal of Atmospheric and Solar-Terrestrial Physics*, *189*, 35–43. https://doi.org/10.1016/j.jastp.2019.04.002

Poluianov, S. V., Usoskin, I. G., Mishev, A. L., Shea, M. A., & Smart, D. F. (2017). GLE and sub-GLE redefinition in the light of high-altitude polar neutron monitors. *Solar Physics*, *292*(11), 176. https://doi.org/10.1007/s11207-017-1202-4

Reagan, J. B., Meyerott, R. E., Evans, J. E., Imhof, W. L., & Joiner, R. G. (1983). The effects of energetic particle precipitation on the atmospheric electric circuit. *Journal of Geophysical Research*, *88*(C6), 3869–3878. https://doi.org/10.1029/jc088ic06p03869

Reiter, R. (1969). Solar flares and their impact on potential gradient and air-Earth current characteristics at high-mountain stations. *Pure and Applied Geophysics*, *72*(1), 259–267. https://doi.org/10.1007/bf00875709

Reiter, R. (1971). Further evidence for impact of solar flares on potential gradient and air-Earth current characteristics at high-mountain stations. *Pure and Applied Geophysics*, *86*(1), 142–158. https://doi.org/10.1007/bf00875081

Rycroft, M. J., Nicoll, K. A., Aplin, K. L., & Harrison, R. G. (2012). Recent advances in global electric circuit between the space environment and the troposphere. *Journal of Atmospheric and Solar-Terrestrial Physics*, *90–91*, 198–211. https://doi.org/10.1016/j.jastp.2012.03.015

Sartor, D. (1980). Electric field perturbations in terrestrial clouds and solar flare events. *Monthly Weather Review*, *198*(4), 499–505. https://doi.org/10.1175/1520-0493(1980)108<0499:efpitc>2.0.co;2

Sheftel, V. M., Bandilet, O. I., Yaroshenko, A. N., & Chernyshev, A. K. (1994). Space-time structure and reasons of global, regional, and local variations of atmospheric electricity. *Journal of Geophysical Research*, *99*(D5), D10797. https://doi.org/10.1029/93jd02857

Sinnhuber, M., Nieder, H., & Wieters, N. (2012). Energetic particle precipitation and the chemistry of the mesosphere/lower thermosphere. *Surveys in Geophysics*, *33*(6), 1281–1334. https://doi.org/10.1007/s10712-012-9201-3

Tacza, J., Raulin, J.-P., Morales, C. A., Macotela, E., Marun, A., & Fernandez, G. (2021). Analysis of long-term potential gradient variations measured in the Argentinian Andes. *Atmospheric Research*, *248*, 105200. https://doi.org/10.1016/j.atmosres.2020.105200

Tacza, J., Raulin, J.-R., Mendonca, R. R. S., Makhmutov, V. S., Marun, A., & Fernandez, G. (2018). Solar effects on the atmospheric electric field during 2010-2015 at low latitudes. *Journal of Geophysical Research: Atmospheres*, *123*(21), 11970–11979. https://doi.org/10.1029/2018jd029121

Takagi, Y., & Iwata, A. (1984). *Solar influence on the Earth's electric field*. paper presented at seventh international conference on atmospheric electricity. American Meteorological Society:Albany, NY.

Vainio, R., Desorgher, L., Heynderickx, D., Storini, M., Fluckiger, E., Horne, R. B., et al. (2009). Dynamics of the Earth's particle radiation environment. *Space Science Reviews*, *147*(3–4), 187–231. https://doi.org/10.1007/s11214-009-9496-7

Willet, J. C. (1979). Solar modulation of the supply current for atmospheric electricity? *Journal of Geophysical Research*, *84*(C8), 4999–5002. https://doi.org/10.1029/jc084ic08p04999

Wu, Q., Li, H., & Wang, C. (2020). Short-term lightning response to ground level enhancements. *Frontiers in Physics*, *8*, 348. https://doi.org/10.3389/fphy.2020.00348